Computer Assisted Mechanics and Engineering Sciences, 5: 21–30, 1998.

A direct block sparse solution of the mixed finite element equations

Mladen Berković
Faculty of Mathematics, P.O. Box 550, 11000 Belgrade, Yugoslavia

Zoran Drašković
Mathematical Institute, P.O. Box 367, 11000 Belgrade, Yugoslavia

Dubravka Mijuca
Faculty of Mathematics, P.O. Box 550, 11000 Belgrade, Yugoslavia

(Received September 30, 1996)

In this paper a practical procedure for the solution of really sized mixed problems, generating a continuous stress field (where appropriate) and having both the stress and displacement boundary conditions exactly satisfied, is described. The system matrix for the present formulation can be subdivided into the blocks, if the field variables (stresses and displacements) are separated for computational purposes. In addition, the structure of these blocks is sparse, similarly as the structure of the stiffness matrix in classical finite element analysis. Block sparse solution procedure, accounting for the pattern of the resulting system matrix is proposed. Computer implementation confirmed feasibility of the described solution procedure. In addition, numerical tests show remarkably high accuracy and convergence rate of the present mixed scheme for both the stresses and displacements. Due to high accuracy of the scheme, it can be competitive in comparison with usual displacement approach, although the count of arithmetic operations for the same mesh density in mixed procedure can be an order of magnitude larger than in classical finite element analysis.

1. Introduction

Contemporary finite elements are usually based on some formulations that can be called 'mixed', in a sense that, at variance with the classical finite element method, where fundamental unknowns are displacements only, here the fundamental variables can be also stresses and/or strains. Primary goal of the present paper is to discuss practical aspects of a rather uncommon mixed formulation, similar in principle to that in Zienkiewicz and Taylor [1] but having both the stress and displacement boundary conditions exactly satisfied. The proposed formulation has been already anticipated in [1, p. 333] as follows: '*It is [...] possible to derive elements that exhibit complete continuity of the appropriate components along interfaces [...] Extension to the full stress problem is difficult and as yet such elements have not been successfully used*'.

To handle the stress components adequately and conveniently, we accommodate [2] the boundary (interface) nodal coordinate surfaces to be coincident or at least tangent to the local boundary surfaces and/or interfaces. Then it is possible, besides the displacement constraints, to treat also the stress constraints as the essential boundary conditions. As it can be concluded on the basis of the existing (iterative) computational evidence of Cantin *et al.* [3], where the stress boundary conditions were satisfied in an iterative manner, such an approach is a very promising way towards improvement of the performances of mixed finite elements.

However, it has been shown that such systems with interpolation functions of the same order for the stresses and displacements, in the general case do not satisfy LBB (Ladyzhenskaya, Babuška, Brezzi) condition, and hence cannot be solved [4]. For the stability of a solution it is necessary to increase the number of the stress degrees of freedom. A reasonable choice for the general use is to add central, bubble nodes, similarly to the usual remedies in the Stokes problem. In the present paper we discuss computational aspects and numerical results of the proposed formulation. It has been already shown in [5] that an algebraic system resulting from the above formulation, looks to be very well suited for the solution by the use of the so-called 'natural factor' approach, proposed by Argyris *et al.* [6].

2. Mathematical model

We use the weak formulation of a mixed problem, associated with the mixed (Reissner's) variational principle [7] and equivalent to the formulation of Zienkiewicz and Taylor [1]:

Find $\boldsymbol{T} \in \boldsymbol{T}^2$ and $\boldsymbol{u} \in \boldsymbol{H}^1$ such that $\boldsymbol{u}|_{\partial\mathcal{B}_u} = \boldsymbol{w}$ and

$$\int_{\mathcal{B}} (\boldsymbol{S}{:}\boldsymbol{A}{:}\boldsymbol{T} - \boldsymbol{S}{:}\nabla\boldsymbol{u} - \nabla\boldsymbol{v}{:}\boldsymbol{T})\,\mathrm{d}V = -\int_{\mathcal{B}} \boldsymbol{v}\cdot\boldsymbol{f}\,\mathrm{d}V - \int_{\partial\mathcal{B}_t} \boldsymbol{v}\cdot\boldsymbol{p}\,\mathrm{d}A \tag{1}$$

for all $\boldsymbol{S} \in \boldsymbol{T}^2$ and $\boldsymbol{v} \in \boldsymbol{H}^1$ such that $\boldsymbol{v}|_{\partial\mathcal{B}u} = \boldsymbol{0}$.

In this expression $\boldsymbol{T}$ is the stress tensor, $\boldsymbol{f}$ the vector of the body forces, $\boldsymbol{u}$ the displacement vector, $\boldsymbol{A}$ the elastic compliance tensor, $\boldsymbol{p}$ the vector of the boundary tractions, and $\boldsymbol{w}$ the vector of the prescribed displacements. Further, $\boldsymbol{T}^2$ is the space of all square integrable symmetric tensor fields while $\boldsymbol{H}^1$ is the space of all vector fields that are square integrable and have square integrable gradient. Finally, $\mathcal{B}$ is an open, bounded domain of the elastic body, $\boldsymbol{n}$ is the unit normal vector to the boundary $\partial\mathcal{B}$, while $\partial\mathcal{B}_t$ and $\partial\mathcal{B}_u$ are the portions of $\partial\mathcal{B}$ where the stresses or the displacements are prescribed, respectively.

3. Finite element approximation

We let $\mathcal{C}_h$ be the partitioning of $\mathcal{B}$ into elements $\mathcal{E}$ and define the finite element subspaces for the displacement vector, the stress tensor and the appropriate weight functions respectively as

$$\boldsymbol{U}_h = \left\{\boldsymbol{u} \in \boldsymbol{H}^1(\mathcal{B}) \mid \boldsymbol{u}|_{\partial\mathcal{B}_u} = \boldsymbol{w}, \quad \boldsymbol{u}|_{\mathcal{E}} = U^K(\mathcal{E})\,\boldsymbol{u}_K, \quad \forall\mathcal{E} \in \mathcal{C}_h\right\}, \tag{2}$$

$$\boldsymbol{T}_h = \left\{\boldsymbol{T} \in \boldsymbol{T}^1(\mathcal{B}) \mid \boldsymbol{T}\boldsymbol{n}|_{\partial\mathcal{B}_t} = \boldsymbol{p}, \quad \boldsymbol{T}|_{\mathcal{E}} = T_L(\mathcal{E})\,\boldsymbol{T}^L, \quad \forall\mathcal{E} \in \mathcal{C}_h\right\}, \tag{3}$$

$$\boldsymbol{V}_h = \left\{\boldsymbol{v} \in \boldsymbol{H}^1(\mathcal{B}) \mid \boldsymbol{u}|_{\partial\mathcal{B}_u} = \boldsymbol{0}, \quad \boldsymbol{v}|_{\mathcal{E}} = V^M(\mathcal{E})\,\boldsymbol{v}_M, \quad \forall\mathcal{E} \in \mathcal{C}_h\right\}, \tag{4}$$

$$\boldsymbol{S}_h = \left\{\boldsymbol{S} \in \boldsymbol{T}^1(\mathcal{B}) \mid \boldsymbol{S}\boldsymbol{n}|_{\partial\mathcal{B}_t} = \boldsymbol{0}, \quad \boldsymbol{S}|_{\mathcal{E}} = S_L(\mathcal{E})\,\boldsymbol{S}^L, \quad \forall\mathcal{E} \in \mathcal{C}_h\right\}. \tag{5}$$

In these expressions $\boldsymbol{u}_K$ and $\boldsymbol{T}^L$ are the nodal values of the vector $\boldsymbol{u}$ and tensor $\boldsymbol{T}$ respectively. Accordingly, U^K and T_L are the corresponding values of the interpolation functions, connecting the displacements and stresses at an arbitrary point in $\mathcal{E}$ (the body of an element), and the nodal values of these quantities. The complete analogy holds for the displacement and stress variations (weight functions) $\boldsymbol{v}$ and $\boldsymbol{S}$ respectively.

4. Compact matrix form of the finite element equations

It has been shown in [2] that the problem under consideration can be formulated as

$$\mathbf{At} - \mathbf{Du} = \mathbf{0}, \qquad \mathbf{D}^t\mathbf{t} = \mathbf{F} + \mathbf{P}. \tag{6}$$

In these expressions the nodal stress t^{Lst} and displacement u_{Kq} components are consecutively ordered in the column matrices t and $\mathbf{u}$ respectively. The members of the matrices $\mathbf{A}$ and $\mathbf{D}$ and of the vectors (column matrices) $\mathbf{F}$ and $\mathbf{P}$ (discretized body and surface forces) are respectively:

$$A_{NuvLst} = \sum_e \int_{\mathcal{E}} S_N\, g^a_{(N)u}\, g^b_{(N)v}\, A_{abcd}\, g^c_{(L)s}\, g^d_{(L)t}\, T_L \;\mathrm{d}V\,, \tag{7}$$

$$D^{Kq}_{Nuv} = \sum_e \int_{\mathcal{E}} S_N U^K_a\, g^a_{(N)u}\, \mathrm{d}V\, g^{(K)q}_{(N)v}\,, \tag{8}$$

$$F^{Mq} = \sum_e \int_{\mathcal{E}} g^{(M)q}_a V^M f^a\, \mathrm{d}V\,, \tag{9}$$

$$P^{Mq} = \sum_e \int_{\partial\mathcal{E}_t} g^{(M)q}_a V^M p^a\, \mathrm{d}A\,, \tag{10}$$

where

$$g^{(K)m}_{(L)s} = \delta_{kl}\, g^{(K)mn} \frac{\partial z^k}{\partial x^{(K)n}} \frac{\partial z^l}{\partial y^{(L)s}}\,, \tag{11}$$

$$g^a_{(L)s} = \delta_{kl}\, g^{ab} \frac{\partial z^k}{\partial \xi^b} \frac{\partial z^l}{\partial y^{(L)s}}\,, \tag{12}$$

$$g^{(K)q}_b = \delta_{kl}\, g^{(K)qp} \frac{\partial z^k}{\partial \xi^b} \frac{\partial z^l}{\partial x^{(K)p}}\,, \tag{13}$$

are the Euclidean shifters. In these expressions z^i $(i,j,k,l = 1,2,3)$ are the global Cartesian coordinates, while $x^{(K)n}$ $(m,n,p,q = 1,2,3)$ and $y^{(L)s}$ $(r,s,t,u,v = 1,2,3)$ are local (nodal) coordinates, used for determination of the nodal displacements and stresses respectively. Commonly used notions, ξ^a $(a,b,c,d = 1,2,3)$ are taken for the local (element) coordinates, usually convected (parametric, isoparametric). Further, $g^{(K)mn}$ and g^{ab} are the components of the contravariant fundamental metric tensors, the first one with respect to $x^{(K)n}$ and the second to ξ^b. Computation of these quantities is described in detail per instance in [2]. Furthermore, $U^K_a = \partial U^K / \partial \xi_a$. Finally, A_{abcd} are the components of the elastic compliance tensor $\boldsymbol{A}$, while f^a and p^a are the body forces and boundary tractions, respectively. Integration is performed over the body $\mathcal{E}$ of each element, or over the part of the boundary surface $\partial\mathcal{E}_t$ where the tractions are given, while summation is over all the elements e of a system.

4.1. Remarks on the solvability

When solvability of (6) is considered, Brezzi's theorem [7] is often cited. Instead of going into the details of this theorem, we elaborate here only its algebraic implications. First of all, in the analysis of the regular mixed $(\boldsymbol{T}, \boldsymbol{u})$ formulation (1) of the elasticity problem, the first condition of the aforementioned theorem can be ascertained [4]. Hence, the second or LBB condition remains to be satisfied. In the accordance with Oden [8, p. 134], if LBB is to hold, so also must a condition on the rank of $\mathbf{D}$, i.e.

$$\mathbf{Du} = \mathbf{0} \text{ implies that } \mathbf{u} = \mathbf{0}. \tag{14}$$

This means that we should have

$$\dim \boldsymbol{T}_h \geq \dim \nabla \boldsymbol{U}_h, \tag{15}$$

where

$$\nabla \boldsymbol{U}_h = \left\{ 2\boldsymbol{e}_h = \nabla \boldsymbol{u}_h + \nabla \boldsymbol{u}^t_h, \quad \boldsymbol{u}_h \in \boldsymbol{U}_h \right\} \tag{16}$$

is evidently a *strain* subspace. Let us discuss now the dimensions (number of entries) of the spaces under consideration. In the absence of the boundary conditions, and if the same mesh is used for both the displacements and stresses, taking also into account the symmetry of the strain and stress tensors, the dimensions of the displacement, strain and stress spaces will be respectively:

$$\begin{aligned} n_u &= \dim \boldsymbol{U}_h = nN_u \,; \\ n_t &= \dim \boldsymbol{T}_h = \frac{1}{2}n\,(n+1)\,N_t \,; \\ n_e &= \dim \nabla \boldsymbol{U}_h = \frac{1}{2}n\,(n+1)\,N_u \,. \end{aligned} \tag{17}$$

Certainly, $\boldsymbol{T}_h$ and $\nabla\boldsymbol{U}_h$ are the spaces of the second order tensors. Each of these tensors has $n\,(n+1)\,/2$ components, where n is the total number of spatial dimensions of the problem under consideration. Furthermore, N_t is the number of nodes of a *stress mesh*, while N_u is the number of nodes of a *displacement mesh.* From (15) and (17) it follows directly that, in the absence of the stress boundary conditions, the rank condition (14) will be satisfied if

$$N_t \geq N_u. \tag{18}$$

This relationship justifies the success of the scheme described in [5], where $N_t = N_u$.

Let us note also that, because at each node of a stress mesh we have (due to the symmetry of a stress tensor) $n\,(n+1)\,/2$ stress degrees of freedom, and at each node of a displacement mesh n displacement degrees of freedom, the well-known condition:

$$n_t \geq n_u \,, \tag{19}$$

(see per instance [1]), can be rewritten as

$$\frac{1}{2}n\,(n+1)\,N_t \geq nN_u \,. \tag{20}$$

If (18) holds, (20) will be satisfied for any and every value of n. However, the reverse is not true. Consequently, (18) is a stronger condition than (19) and hence more helpful in giving ideas how to construct and modify the trial space to maintain solvability. Furthermore, if (some or all) of the stress boundary conditions are enforced, (18) can be replaced by a somewhat conservative heuristic rule

$$N_t - N_t^* \geq N_u \,. \tag{21}$$

In this expression, N_t^* is the number of nodes having at least one of the stress components prescribed. It is evident that (21) cannot be satisfied for $N_t = N_u$, i.e. if the same mesh is used for both the displacements and stresses. Hence it is necessary to enrich the stress mesh by the additional nodes. More details will be given in the discussion on the numerical example.

4.2. Effective solution of a system

As it has been shown in [2], a suitable choice of the local boundary coordinate systems enables us to find one-to-one correspondence between the prescribed boundary tractions and some of the stress components, i.e. $\mathbf{t}_p$ (prescribed) at a boundary.

$$\begin{bmatrix} \mathbf{A}_{vv} & -\mathbf{D}_{vv} \\ -\mathbf{D}_{vv}^{\mathrm{t}} & \mathbf{0} \end{bmatrix} \begin{bmatrix} \mathbf{t}_v \\ \mathbf{u}_v \end{bmatrix} = \begin{bmatrix} -\mathbf{A}_{vp} & \mathbf{D}_{vp} \\ \mathbf{D}_{pv}^{\mathrm{t}} & \mathbf{0} \end{bmatrix} \begin{bmatrix} \mathbf{t}_p \\ \mathbf{u}_p \end{bmatrix} - \begin{bmatrix} \mathbf{0} \\ \mathbf{F}_p + \mathbf{P}_p \end{bmatrix}. \tag{22}$$

In this expression unknown (variable) stresses $\mathbf{t}_v$ and displacements $\mathbf{u}_v$, and the known (prescribed) ones $\mathbf{t}_p$ and $\mathbf{u}_v$, are separated. Further, $\mathbf{F}_p$ and $\mathbf{P}_p$ are the prescribed discretized body and surface forces respectively, the same as in the classical finite element analysis.

The problem considered in this paper has a regular symmetric matrix $\mathbf{A}_{vv}$, and hence can be solved, per instance, by the symmetric solver described in [5]. After the solution of the first row in (22) for $\mathbf{t}_v$, and the replacement of this result into the second one, we obtain the matrix equation

$$\mathbf{D}^t_{vv}\mathbf{A}^{-1}_{vv}\mathbf{D}_{vv}\mathbf{u}_v = \mathbf{R}, \tag{23}$$

where

$$\begin{aligned} \mathbf{R} &= -\mathbf{R}_2 - \mathbf{D}^t_{vv}\mathbf{A}^{-1}_{vv}\mathbf{R}_1\,, \\ \mathbf{R}_1 &= \mathbf{D}_{vp}\mathbf{u}_p - \mathbf{A}_{vp}\mathbf{t}_p\,, \\ \mathbf{R}_2 &= \mathbf{D}^t_{pv}\mathbf{t}_p - \mathbf{F}_p - \mathbf{P}_p\,. \end{aligned} \tag{24}$$

The global flexibility matrix can be transformed, e.g. by the use of the fast Givens transformation [5, 6] or Gaussian triangularization procedure [10] to a form

$$\mathbf{A}_{vv} = \mathbf{U}^t\mathbf{T}\mathbf{U}. \tag{25}$$

In this expression, $\mathbf{T}$ is a diagonal matrix, while $\mathbf{U}$ is an upper triangular invertible matrix. Hence, the system (23) can be rewritten as

$$\mathbf{H}^t\mathbf{E}\mathbf{H}u_v = \mathbf{R}, \qquad \mathbf{R} = -\mathbf{R}_2 - \mathbf{H}^t\mathbf{E}\mathbf{V}. \tag{26}$$

In this expression $\mathbf{H}$, $\mathbf{V}$ and $\mathbf{E}$ are defined by the relationships

$$\mathbf{U}^t\mathbf{H} = \mathbf{D}_{vv}, \qquad \mathbf{U}^t\mathbf{V} = \mathbf{R}_1, \qquad \mathbf{E} = \mathbf{T}^{-1}. \tag{27}$$

It should be noted again that $\mathbf{U}^t$ is a lower triangular, and $\mathbf{T}$ is a diagonal matrix. Consequently, calculations (27) are relatively simple and fast. Moreover, because $\mathbf{U}^t$ is lower triangular, the initial sparse structure of $\mathbf{D}_{vv}$ is retained. Hence, troublesome inversion of $\mathbf{A}_{vv}$ [9, p. 74] is not only unnecessary. In fact, its avoidance enables us to construct a competitive computational scheme for the solution of (22).

Finally, it is very important to recognize that $\mathbf{H}^t\mathbf{E}\mathbf{H}$ is nothing else than a stiffness matrix. If only a part of structure is modeled by mixed elements, there is no obstacle to merge $\mathbf{H}^t\mathbf{E}\mathbf{H}$ with other stiffness matrices in any finite element system having an option of user defined element. Also, it can be conveniently transformed either by Gaussian triangularization (after the assembly procedure), or directly by the fast Givens procedure (natural factor formulation [6]). Without going into the further details, let us say only that computational experience of the present authors indicates, at least for the systems under consideration, that Gaussian elimination looks to be a more stable procedure.

5. Stress computations

5.1. Scheme 1

From (24), (25) and (27) it follows that the stresses can be determined by the solution of the triangular system in which all the matrices are already known:

$$\mathbf{U}\mathbf{t}_v = \mathbf{E}\left[\mathbf{V} + \mathbf{H}\mathbf{u}_v\right]. \tag{28}$$

5.2. Scheme 2

An alternative approach is, after finding unknown displacements from (26), to abandon the additional (usually bubble) nodes, and to consider all remaining (even prescribed) stresses as unknowns. Stresses can be now determined from the system

$$\mathbf{At} = \mathbf{Du}. \tag{29}$$

i.e. (6a). This system also can be reduced to a form similar to (28), but simpler:

$$\mathbf{U}_0\mathbf{t} = \mathbf{E}_0\mathbf{H}_0\mathbf{u}. \tag{30}$$

Note also that the matrices $\mathbf{U}_0$, $\mathbf{E}_0$ and $\mathbf{H}_0$ can, from the computational point of view, be determined in the same pass when $\mathbf{U}$, $\mathbf{E}$ and $\mathbf{H}$. The difference is only due to the rows and columns of these matrices, inactive in the relationships (25)–(28) or in (30).

6. Plane stress problem

Numerical experiments will be conducted for the plane stress problem. A model with the stress boundary conditions satisfied as the essential ones and N_t increased to satisfy (21) by a central, 'bubble' node along with the basic bilinear stress distribution in the quadrilateral isoparametric elements is studied.

The problem under consideration, borrowed from [11], (Fig. 1) is a square plate of the unit semispan, with a central circular hole of the unit diameter. The plate is loaded along its sides by the unit load, tensile in horizontal, and compressive in vertical directions. Modulus of elasticity and Poisson's coefficient are taken to be $E = 1$ and $\nu = 0.3$ respectively. Local coordinate systems for the determination of the stresses at nodes situated along AC on Fig. 2 are local Cartesian, having one axis tangential and other orthogonal to the interior contour circle at a boundary node. For the convergence estimate we use the stress value t= t^{xx} at a point C, which is positive and hence equals the supreme norm (because of the supreme value of the stress at that point), and the local

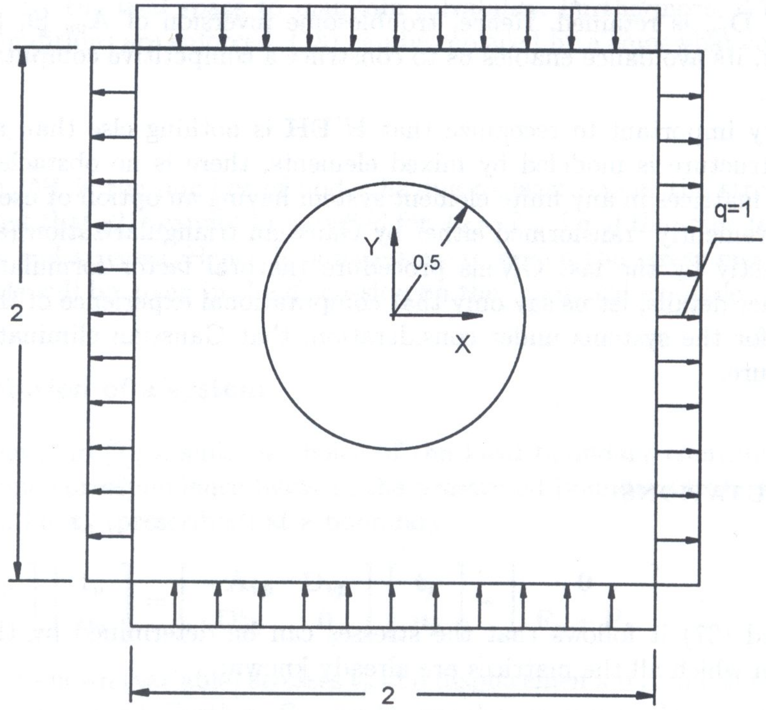

Fig. 1. Plate with a circular hole

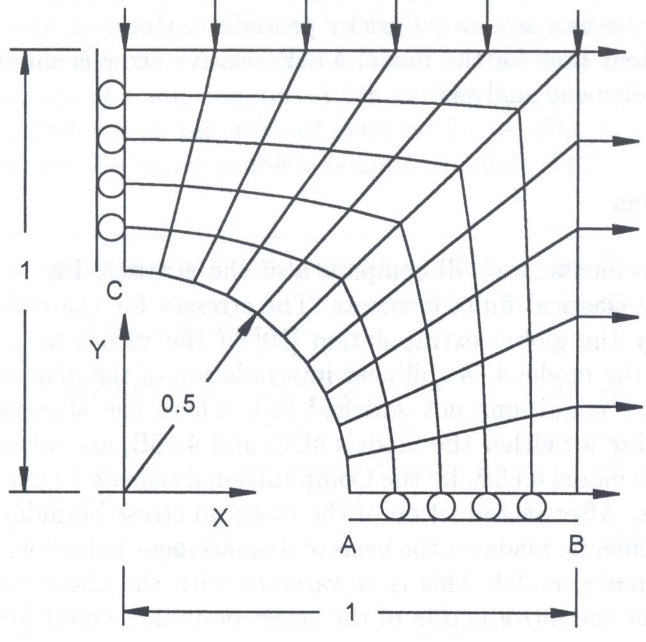

Fig. 2. Finite element mesh

displacement value u= u_x at a point A, also greater than zero and close to the largest displacement (point B). Converged values of this stress and displacement are approximately t= 10.39 and u= 6.09.

6.1. Displacement calculations

For the comparison of the present results with the standard finite element ones, the first (lowest) curve on Fig. 3 correspond to a bilinear isoparametric four node element, labeled by 4DIS. The next curve, labeled by 4+4, corresponds to a standard mixed finite element procedure with bilinear and continuous at the element interfaces both the displacements and stresses [5]. The present model, with the stress boundary conditions satisfied as the essential ones and N_t increased to satisfy (21) by only a bubble mode of the second-order stress distribution, is shown at a curve 4+5B. A

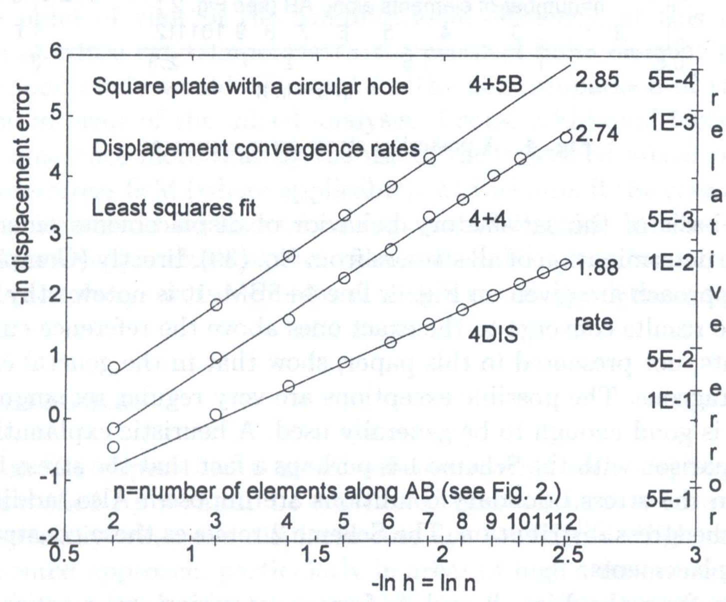

Fig. 3. A posteriori displacement error estimates

posteriori convergence rate in this case approaches 3. Certainly, finding the convergence rates from a posteriori error estimates is a somewhat tricky procedure. However, the relative error is a value one can trust. It is evident that for the model 4+5B relative error is smaller orders of magnitude than for classical finite element analysis.

6.2. Stress calculations

Similarly as the displacements, we will compare also the stresses, Fig. 4, before of all with the standard results for the classical finite elements. The stresses for the classical model denoted by 4DIS are determined by the global extrapolation [10] of the values from the element centroids. Further, the results for the model 4+4 (bilinear interpolation of the displacements and continuous stresses, stress boundary conditions not satisfied [5]), where the stresses are uniquely defined, without dilemmas existing for either the models 4DIS and 4+5B, are taken for the reference ones. The stress results for the model 4+5B, by the Computational scheme 1 (Fig. 4), are not so flattering as for the displacements. After introduction of the essential stress boundary conditions, and other aforementioned improvements, made on the basis of displacement behavior, the results are generally worse than for the reference model. This is at variance with the above results for displacements, which are improved after the introduction of the stress boundary conditions.

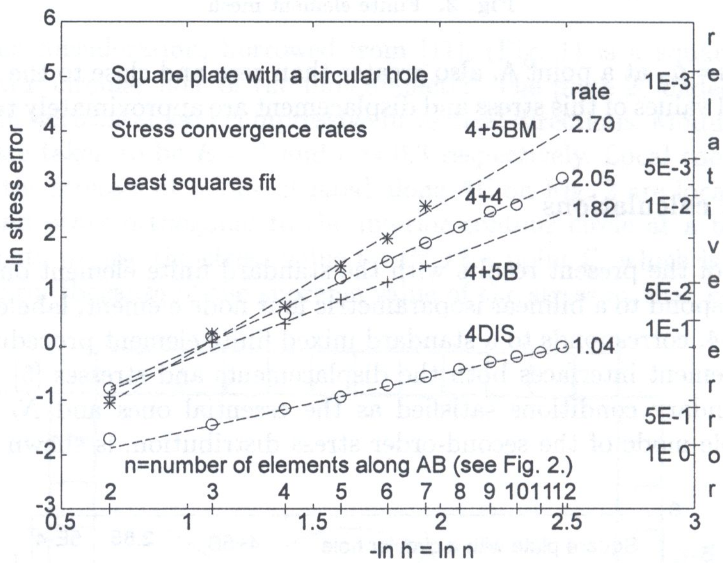

Fig. 4. A posteriori stress error estimates

However, on the basis of the satisfactory behavior of displacements emerged an idea to use displacements for the determination of all stresses from Eq. (30) directly (Computational scheme 2). The results of this approach are given on Fig. 4, line 4+5BM. It is noteworthy that, in contrary to the previous case, the results converge to the exact ones above the reference curve 4+4. Additional numerical experiments, not presented in this paper, show that in the general case Scheme 2, given by Eq. (30) is advantageous. The possible exceptions are very regular rectangular meshes. Even in such cases Scheme 2 is good enough to be generally used. A heuristic explanation of the success of Scheme 2 in the comparison with the Scheme 1 is perhaps a fact that the stress field is in some sense overconstrained when the stress boundary conditions are imposed. Also, additional bubble nodes are likely to deform the stress distribution. The Scheme 2 removes these constraints, calculating all stresses from the displacements.

As it can be seen from the Figs. 3 and 4, from a posteriori error estimates it follows that convergence rates for both the displacements and stresses approach $r = 3$, at least for this particular example. Hence, one can speak about superconvergence. A possible explanation of this behavior is that we apply stronger continuity than required for the underlying variational principle. However, this behavior of a solution also can be considered as local, in the stress concentration area. For the better insight into the nature of a solution, an additional test has been performed, concerning the convergence in energy, calculated as the work of external forces (Fig. 5) Note that the converged value of the strain energy for the above problem is approximately 3.82.

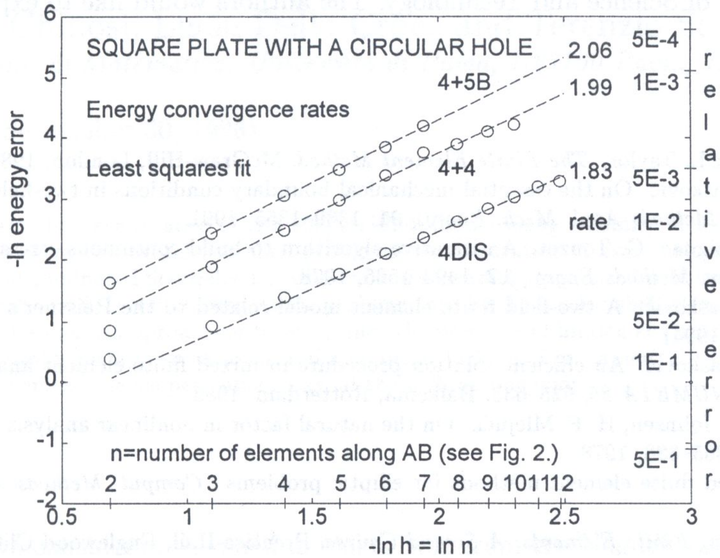

Fig. 5. A posteriori energy error estimates

Not surprisingly, the convergence in energy is almost exactly quadratic for all models, as it should be expected on the basis of a priori error estimates for bilinear finite element subspaces. However, the accuracy is definitively in favor of the mixed model with the stress boundary conditions exactly satisfied. For the same displacement mesh, the relative error is almost an order of magnitude smaller than for standard finite element analysis.

But, some preliminary calculations show that the number of arithmetic operations can be an order of magnitude larger than in the classical finite element analysis over the same mesh.

Hence, from the point of view of the computational efficiency, at this moment one can say that the described procedure can compete with the classical finite element analysis, and that an additional more detailed study would be useful for the fair comparison of these two approaches. Such a study can be in favor of the mixed analysis, if some additional facts are also considered. Before of all, let us note once more that by the use of the described mixed procedure, we already construct a continuous stress field (where applicable). At variance, if the classical approach is used, the postprocessing price should be also taken into account, which can be even higher than for the basic analysis. Moreover, in classical finite element analysis, the convergence in energy of the smoothed stress fields is always worse, compared with a raw finite element solution [12].

7. Concluding remarks

It has been shown in the paper that a mixed scheme having both displacement and boundary traction conditions satisfied *a priori*, can be orders of magnitude more accurate than classical finite element analysis, especially when the displacements are considered. High convergence rates and accuracy of the presented approach, particularly in areas of high stress concentration, recommend it for the further research, despite the larger and more complex system of equations than in classical finite element analysis. A solution procedure accounting for a block and sparse pattern of the resulting system matrix is proposed. This procedure makes the aforementioned mixed scheme competitive in comparison with the classical finite element analysis.

ACKNOWLEDGEMENT

This work has been carried out within the framework of the projects 04M03 and 04M01 sponsored by the Serbian Ministry of Science and Technology. The authors would like to express their gratitude.

REFERENCES

[1] O.C. Zienkiewicz, R.L. Taylor, *The Finite Element Method.* McGraw-Hill, London, 1989.

[2] M. Berković, Z. Drašković. On the essential mechanical boundary conditions in two-field finite element approximations, *Comput. Methods Appl. Mech. Engrg.*, **91**: 1339–1355, 1991.

[3] G. Cantin, G. Loubignac, G. Touzot. An iterative algorithm to build continuous stress and displacement solutions. *Int. J. Numer. Methods Engrg.*, **12**: 1493–1506, 1978.

[4] M. Berković, Z. Drašković. A two-field finite element model related to the Reissner's principle. *Theor. Appl. Mech.*, **20**: 17–36, (1994).

[5] M. Berković, Z. Drašković. An efficient solution procedure in mixed finite element analysis. In: J. Middleton, G.N. Pande, eds., *NUMETA 85*, 625–633. Balkema, Rotterdam, 1985.

[6] J.H. Argyris, Th.L. Johnsen, H.-P. Mlejnek. On the natural factor in nonlinear analysis *Comput. Methods Appl. Mech. Engrg.*, **15**: 365–388, 1978.

[7] D.N. Arnold, Mixed finite element methods for elliptic problems. *Comput. Methods Appl. Mech. Engrg.*, **82**: 281–300, 1990.

[8] G. Carey, J.T. Oden. *Finite Elements: A Second Course.* Prentice-Hall, Englewood Cliffs, 1983.

[9] F. Brezzi, M. Fortin. *Mixed and Hybrid Finite Element Methods.* Springer–Verlag, New York, 1991.

[10] D. Mijuca, M. Berković. Some stress recovery procedures in the classical finite element analysis. *Proc. XXI Yugoslav Congress of the Theoretical and Applied Mechanics C5-87*, 512–517. Niš, 1995.

[11] A.K. Rao, I.S. Raju, A.V. Krishna Murty. A powerful hybrid method in finite element analysis. *Int. J. Numer. Methods Engrg.*, **3**: 389–403, 1971.

[12] D. Mijuca, Z. Drašković, M. Berković. Displacement based continuous stress recovery procedure. *CST 96, The Third Int. Conf. on Computational Structures Technology.* Budapest, 1996.